Transformation behaviors, structural and magnetic characteristics of Ni–Mn–Ga films on MgO (001)*

Xie Ren(谢 忍), Tang Shao-Long(唐少龙)†, Tang Yan-Mei(唐妍梅), Liu Xiao-Chen(刘枭辰), Tang Tao(唐 涛), and Du You-Wei(都有为)

National Laboratory of Microstructures, Jiangsu Provincial Laboratory for Nanotechnology and Department of Physics, Nanjing University, Nanjing 210093, *China*

(Received 14 May 2013; revised manuscript received 7 June 2013)

Ferromagnetic Ni–Mn–Ga films were fabricated by depositing on MgO (001) substrates at temperatures from 673 K to 923 K. Microstructure, crystal structure, martensitic transformation behavior, and magnetic properties of the films were studied. With increasing deposition temperature, the surface morphology of the films transforms from granular to continuous. The martensitic transformation temperature is not dependent on deposition temperature; while transformation behavior is affected substantially by deposition temperature. X-ray analysis reveals that the film deposited at 873 K has a 7M martensite phase, and its magnetization curve provides a typical step-increase, indicating the occurrence of magnetically induced reorientation (MIR). *In situ* magnetic domain structure observation on the film deposited at 873 K reflects that the martensitic transformation could be divided into two periods: nucleation and growth, in the form of stripe domains. The MIR occurs at the temperature at which martensitic transformation starts, and the switching field increases with the decrease of temperature due to damped thermal activation. The magnetically induced martensitic transformation is related to the difference of magnetization between martensite and austenite. A shift of martensite temperature of $\mathrm{d}T/\mathrm{d}H = 0.43$ K/T is observed, consistent with the theoretical value, 0.41 K/T.

Keywords: Ni–Mn–Ga film, ferromagnetic-shape memory alloy, transformation behavior, magnetically induced reorientation, magnetically induced martensitic transformation

PACS: 75.70.Ak, 75.70.Kw **DOI:** 10.1088/1674-1056/22/10/107502

1. Introduction

Ferromagnetic-shape memory alloy Ni–Mn–Ga belongs to a class of advanced multifunctional magnetic materials with attractive properties technological uses, for example, ferromagnetic-shape memory effect,[1] superelasticity,[1] large negative magneto-resistivity,[2,3] giant magneto-caloric effect,[4,5] magnetic-field-induced strain,[5–8] etc., which can be exploited for sensors, actuators, magnetic refrigeration, and other attractive applications in magnetic field measurement systems, in roles that cannot be fulfilled by other shape memory materials.

Among those exciting properties, magnetic-field-induced strain has become a major research subject because large reversible magnetostrains up to 10%[8] can be produced by a field activation frequency on the order of 1.5 kHz.[9,10] Such large strain output and high frequency response of Ni–Mn–Ga materials are determined by the magnetically induced reorientation (MIR) of twin martensite variants through the motion of the twin boundaries under an external magnetic field if the magnetic stress is in excess of the twinning stress. An alternative actuation mode is related to the magnetically induced martensitic transformation (MIM) effect. In a magnetic field, the phase with the higher magnetization is energetically favored; thus, the difference of magnetization between martensite and austenite gives rise to a shift of the martensitic transformation temperature.[11] In the vicinity of the martensitic phase transition temperature, this MIM can be used for actuation.

To develop the unique properties of Ni–Mn–Ga alloys in micro- and nano-system applications like micro-electro–mechanical systems (MEMS),[11–14] researchers around the world are devoted to the preparation and study of Ni–Mn–Ga films. Fabrication of Ni–Mn–Ga alloy in the film form with superior ductility also overcomes the constraints that limit its potential applications to a large extent in its bulk form, that is, high brittleness, low mechanical strength, and poor processability.[14–17] The ductility of Ni–Mn–Ga film is found to be superior to that of the bulk alloy.[18,19] Magnetic sputtering is developed as the mainstream fabrication techniques among PLD[20] and MBE[21,22] to produce Ni–Mn–Ga films, enabling them to be employed in micro- and nano-actuators without fracture failure under deformation. Based on these developments, Ni–Mn–Ga films have already been successfully implemented in prototype microvalves and microscanners.[23,24]

For the Ni–Mn–Ga alloy to realize MIR, the key conditions are: ferromagnetic behavior and the presence of modulated martensitic phase (in the majority of cases, 5

*Project supported by the National Key Project of Fundamental Research of China (Grant No. 2012CB932304), the National Natural Science Foundation of China (Grant No. 50831006), and the Priority Academic Program Development of Jiangsu Higher Education Institutions.

†Corresponding author. E-mail: tangsl@nju.edu.cn

© 2013 Chinese Physical Society and IOP Publishing Ltd

or 7 layered);[25] while for the alloy to be used for MIM and magneto–caloric applications, a well-defined martensitic transformation with transformation hysteresis as narrow as possible is required. Hence, study of the transformation behavior of Ni–Mn–Ga film is very important for its application. As in the Ni–Mn–Ga bulk, the transformation behavior of Ni–Mn–Ga film is very sensitive to its composition. Not only the martensitic transformation temperatures but also the crystal structures of the martensitic phase are closely related to the composition of the films. Wang *et al.*[14] achieved seven-layered modulated martensitic phase with the martensitic starting temperature up to 439 K in an Ni–Mn–Fe–Ga film. On the other hand, the transformation behavior as well as the structural and magnetic properties of Ni–Mn–Ga films were thickness-[26,27] and substrate-dependent,[28] resulting from the residual stress between the substrate and the film; it has also been reported that martensitic transformation could be induced by external magnetic field[29] and stress.[30,31] In addition, sputtering parameters, pressure,[32] and power,[33] have significant influences on the transformation behavior of Ni–Mn–Ga film.

In the present work, the effect of deposition temperature on the structural and magnetic properties, especially the transformation behaviors, of the Ni–Mn–Ga films is analyzed. The film with a 7M martensitic structure is selected for further research; its transformation process is observed by *in situ* evolution of magnetic domain structure. Further, two main actuation modes with potential application as microactuators, magnetically induced reorientation, and magnetically induced martensitic transition, which coexist in this film, are studied.

2. Experiments

Ni–Mn–Ga films were prepared on MgO (001) single-crystalline substrates at deposition temperatures of 673, 773, 873, and 923 K under 0.3 Pa by direct current magnetron sputtering. A sputtering $2''$ target, with a nominal composition of $Ni_{52}Mn_{24}Ga_{24}$, was wire-electrode cut from an ingot which was induction-melted with high-purity elements three times to become homogeneous. A base pressure of better than 2×10^{-5} Pa was achieved to avoid the oxidation of the films, high purity argon atmosphere was introduced during sputtering; the substrate-to-target distance was 6.5 cm; and the sputtering power was maintained at 100 W, resulting in a growth rate of 0.74 nm/s. The 900-nm thickness of the films was controlled by sputtering time and confirmed by a step profiler.

The surface morphology of the films was observed employing a field emission gun scanning electron microscope (SEM, Hitachi S-4800) with a Thermo System 7 EDS spectrometer. The compositions of the films were determined by EDS with an accuracy of 0.5 at.%. X-ray diffraction (XRD, Panalytical X'Pert PRO type) with Cu–K_α radiation was employed to analyze the crystallographic structure of the films by means of grazing incidence in the range of 35°–55°. Magnetization curves were measured using a vibrating sample magnetometer (VSM, Lakershore) in the range of –1.4 T to 1.4 T. Thermomagnetization curves were carried out by superconducting quantum interference device (SQUID, quantum design) to determine the transformation temperatures as well as Curie temperatures of the films. The atomic force microscopy (AFM) and magnetic force microscopy (MFM) observations were performed with a commercial scanning probe microscope (SPM, Veeco diDimension V). A permanent magnet was attached to the bottom of the specimens to provide a magnetic field of 0.12 T normal to the film plane. Topographic (height contrast) and magnetic (phase contrast) images were obtained in tapping and tapping-lift mode, respectively. All the AFM and MFM images were obtained with the scan rate of 0.5 Hz and scan range of 20 μm × 20 μm.

3. Results and discussion

Figure 1 shows the surface morphologies of the Ni–Mn–Ga films deposited at temperatures from 673 K to 923 K. Morphology of the films varies with deposition temperature. The film deposited at low temperature of 673 K is found to be granular structured with oblate grains. When deposition temperature increases to 773 K, grains are instead spherical with a diameter of 100 nm. Whereas the film deposited at the higher temperature of 873 K is found to be continuous with a smooth surface; its surface maximum height (R_{max}) and mean roughness (R_a), obtained by AFM (Fig. 5(a)), are approximately 15.5 nm and 2.1 nm, respectively. The surface of film deposited at 923 K is coarse and rough, with its grain size increasing with deposition temperature, due to atomic consolidation starting from fine grain to coarse grain when deposition temperature levels are moved from low to high. This shows that the increase of deposition temperature induces coarsening in the thin films owing to the increase of grain size and the interconnection of grains.

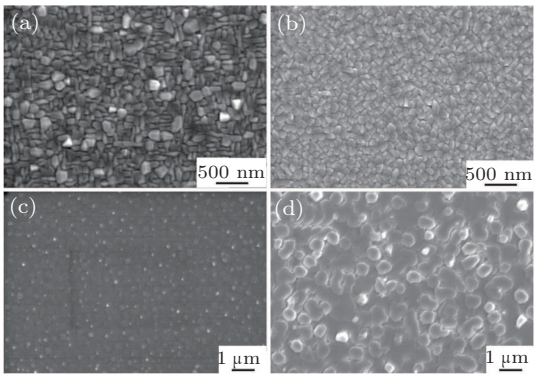


Fig. 1. SEM images of the microstructure of Ni–Mn–Ga films deposited at (a) 673 K, (b) 773 K, (c) 873 K, and (d) 923 K on MgO (001) substrates.

The granular structure does not favor achieving large magnetic field induced strain (MFIS), since the motion of twin boundaries would be constrained by the grain boundary, and the coarse surface of the film deposited at 923 K also does not favor obtaining MFIS.[34,35] It is expected that the continuous and smooth film, the one deposited at 873 K, is structurally favored to obtain a large MFIS.

XRD patterns, recorded at room temperature, of the films deposited from 673 K to 923 K are shown in Fig. 2. To aid clear inspection of the main peaks, the X-ray spectra range of 35°–55° is displayed. Low temperature deposition, 673 K, produces an X-ray spectrum with a weak peak at $2\theta = 44.2°$, identified as (202)/(022) martensitic reflection. Considering the low saturation magnetization of this film (of which magnetization curve is shown in Fig. 4), the film deposited at 673 K is not completely crystallized. Higher deposition temperature, 773 K, gives rise to a considerable increase of the intensity of the X-ray peaks. The X-ray diffraction spectrum for this film exhibits a single sharp peak at $2\theta = 44.2°$, which has been observed previously,[36] indicating a [011]- and/or [101]- oriented martensitic phase. Its crystal structure is extracted to be $a = b > c$, a tetragonal martensite with 5 layers modulation is expected.[37] When the deposition temperature is increased to 873 K, the martensitic peak at $2\theta = 44.2°$ splits into three peaks, which are indentified as (220), (202), and (022) martensitic reflections, respectively. The martensitic {202} peak dominates the polycrystalline diffraction pattern of the films deposited at 773 K and 873 K, suggesting a considerable degree of texture, perhaps a (101) growth mode. Thus, a film/substrate orientational relationship of $(011)[100]_{\text{film}} \parallel (100)[011]_{\text{substrate}}$ is deduced. The three overlapping peaks can be indexed as a (pseudo-) orthorhombic phase with the lattice constants $a = 0.610$ nm, $b = 0.581$ nm, and $c = 0.555$ nm. As deposition temperature increases to 923 K, one can see a tetragonal structure with two peaks with even larger peak splitting, giving a c/a ratio of 1.21, indicating a nonmodulated martensite like that reported in bulk form.[37] This nonmodulated martensitic structure is argued to exhibit no MIR.[25]

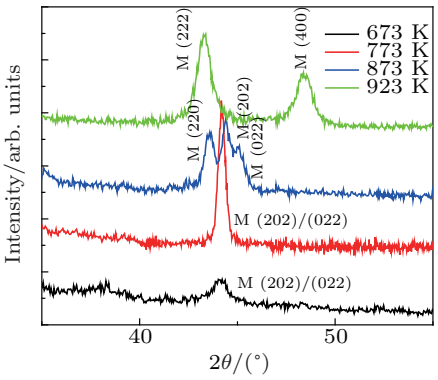


Fig. 2. (color online) XRD spectra, recorded at room temperature, for Ni–Mn–Ga films deposited from 673 K to 923 K.

Thermomagnetization curves, measured under a low magnetic field of 0.01 T parallel to the film plane, for the films deposited from 673 K to 923 K are displayed in Fig. 3 to investigate the transformation behaviors. The martensitic transformation starting (M_s) and finishing (M_f) temperatures during cooling and the austenitic transformation starting (A_s) and finishing (A_f) temperatures during heating as well as Curie temperature are determined by a conventional tangential method and summarized in Table 1. The film deposited at 673 K has a wide martensitic transformation hysteresis, covering the range from 328 K to 303 K. When deposition temperature increases to 773 K, martensitic transformation hysteresis, from 338 K to 286 K, becomes extremely wide; close inspection of the transformation region of the thermomagnetization curve reveals the occurrence of an inter-martensitic transformation (shown in the inset). For the film deposited at 873 K, the hysteresis is drastically reduced to 4 K, which is suitable for MIM applications. As deposition temperature increases to 923 K, magnetization changes abruptly in the vicinity of martensitic transformation, indicating the existence of a large magnetic entropy change, which has the potential to enable realizing a giant magnetocaloric effect. Except for the film deposited at 773 K, no inter-martensitic transformation is observed between 200 K and 400 K in these films. It should be noted that the transformation hysteresis of all the films deposited from 673 K to 923 K are centered around 310 K. The deposition temperature exercises only a minor influence on the martensitic transformation temperature, which is consistent with the fact that the compositions of the films differ little (Table 1), i.e., the volatilization of manganese and gallium are not severe even at high temperatures up to 923 K. However, transformation behavior is profoundly affected by deposition temperature; the evolution of transformation behavior can be ascribed to the atomic order, especially the existence of inter-martensitic transformation.[38] Apparently, the mobility of the atoms depends on the deposition temperature to achieve ordering, as has been reported in bulk.[38,39]

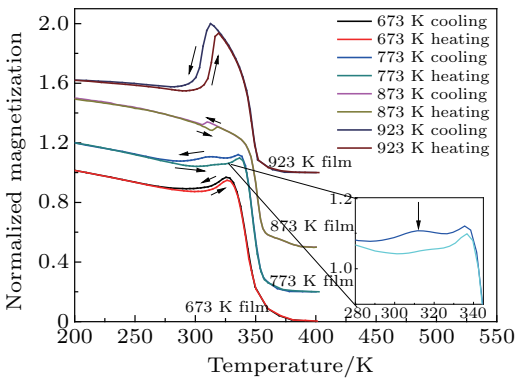


Fig. 3. (color online) Thermomagnetization curves under a magnetic field of 0.01 T parallel to the film plane for Ni–Mn–Ga films deposited at 673, 773, 873, and 923 K on MgO (001) substrates. Inset: details of martensitic transformation for the film deposited at 773 K.

Table 1. Transition temperatures and magnetic properties of Ni–Mn–Ga films deposited at different temperatures.

Depositing temperature/K	Film composition/at.%	T_C/K	M_s/K	M_f/K	A_s/K	A_f/K	S_M/(emu/cc)	$\mu_0 H_c$/T
673	$Ni_{52.5}Mn_{23.8}Ga_{23.7}$	354	328	303	310	329	211	0.0192
773	$Ni_{52.8}Mn_{23.6}Ga_{23.6}$	356	–	–	–	–	263	0.0178
873	$Ni_{52.8}Mn_{23.9}Ga_{23.3}$	358	309	305	313	317	325	0.0204
923	$Ni_{53.1}Mn_{23.4}Ga_{23.5}$	354	312	300	310	318	435	0.0116

Figure 4 demonstrates the magnetization curves, recorded at 300 K, for the films deposited from 673 K to 923 K. These loops were measured in the film plane to avoid the influence of the demagnetization field. The saturation magnetization, S_M, increases with the increase of deposition temperature, resulting from the fact that higher deposition temperature favors crystallization of Ni–Mn–Ga films. The saturation magnetization of the film deposited at 923 K achieves 435 emu/cc, a value compared with bulk martensites. The films deposited at 673, 773, and 923 K provide common single phase loops. While for the film deposited at 873 K, the shape of its magnetization loop changes significantly, and its coercivity increases drastically. Close inspection of the magnetization curve of the film deposited at 873 K (details in the inset) reveals that besides the sharp increase at first, a jump-like step increase occurs at 0.085 T. It has been argued that this typical magnetization behavior originates from MIR.[40–42] This step increase takes place between the fields of 0.087 T and 0.115 T, denoted as H_s and H_f, respectively, where the twin boundary motion occurs. As the field decreases from saturation field, the magnetization goes through a jump-like decrease similar to previous path, but it occurs at lower field, resulting in another hysteresis in the loop. This process indicates that the MIR is reversible.

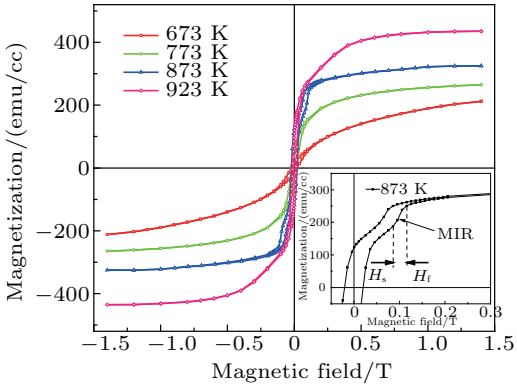


Fig. 4. (color online) M (H) loops recorded at 300 K parallel to the film plane for Ni–Mn–Ga films deposited at 673, 773, 873, and 923 K. Inset: detail of the MIR region of magnetization curve for the film deposited at 873 K.

The 7M martensitic phase, as in the film deposited at 873 K, exhibits an orthorhombic structure with one shortest axis, c axis, which is the easy magnetization axis. When high temperature austenitic phase transforms into martensitic phase, the orientation of the martensitic c axis of this film tends to lie within the film plane to minimize the demagnetization energy, resulting in a featureless domain structure with weak magnetic contrast by MFM for film in the as-deposited state (Fig. 5(b)). On the other hand, direct observation of twin microstructure requires an epitaxial film with an ultra-flat surface.[40,43] For the polycrystalline Ni–Mn–Ga films without surface treatment, twin microstructure could not be directly revealed by surface probe means[14,36] such as AFM (Fig. 5(a)) or SEM (Fig. 1(c)). However, the martensitic c axis is preferably aligned along the direction of external field when the film is cooled with a magnetic field applied. Thus, a magnetic field perpendicular to the film plane is introduced to obtain the visible domain structure with bright and dark contrast by MFM. It is well known that the magnetic domain structure is closely associated to the microstructure,[44,45] allowing us to investigate the twinning structure of the Ni–Mn–Ga films by the evolution of magnetic domain structure.

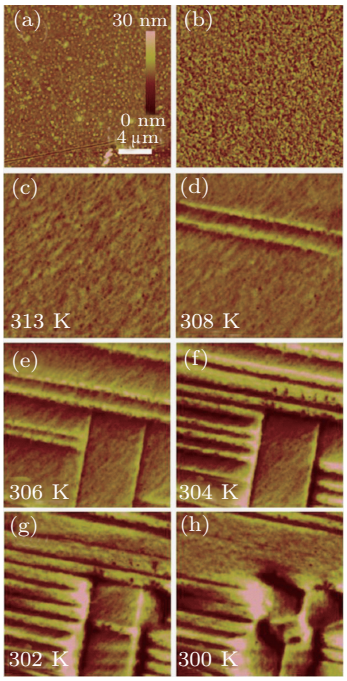


Fig. 5. (color online) (a) AFM and (b) MFM micrographs of the film deposited at 873 K in the as-deposited state. *In situ* domain structure evolution for the film cooling to (c) 313 K, (d) 308 K, (e) 306 K, (f) 304 K, (g) 302 K, and (h) 300 K with a magnetic field of 0.12 T normal to the film plane. All images scanned in the range of 20 μm × 20 μm.

Figure 5 displays the domain structures in the temperature range of 313 K–300 K for the film, deposited at 873 K, cooled with a magnetic field of 0.12 T normal to the film plane. The

magnetic field of 0.12 T is sufficiently high to force the c axis of the nucleated martensite to align perpendicular to the film plane during transformation. Domain structure rarely changes above 309 K, where the film is in the cubic austenitic phase, yielding a featureless MFM image (Fig. 5(c)). At 308 K, two bright domains in the stripe shapes emerge (Fig. 5(d)), consistent with the martensitic transformation starting temperature. It is reasonable to determine that the martensite nucleates in the form of stripe variant. With a decrease of temperature, the number of stripe domains increases, also indicating that the martensite nucleates continuously (Fig. 5(e)). When the temperature decreases to 304 K (Fig. 5(f)), some stripe domains start to grow and become wider. A further decrease of temperature leads to continuous growth of the domains and interconnection of stripe domains (Fig. 5(g)). When the temperature decreases to 300 K, almost all stripe domains are interconnected and the magnetic moments in the entire film are perpendicular to the film plane (Fig. 5(h)). Based on the evolution of domain structure and the correlation between domain structure and the microstructure, the martensitic transformation could be divided into two periods, i.e., nucleation and growth.

$M(H)$ loops for the film deposited at 873 K as a function of temperature are shown in Fig. 6(a). As the $M(H)$ loops are measured in the film plane, the demagnetization factor is negligible. At 360 K, the $M(H)$ loop exhibits the linear response involved with paramagnetic behavior. The slow approach to saturation is ascribed to in the vicinity of the Curie temperature. Cooling to 315 K, the loop is square-like with very small coercivity, resulting in the soft magnetic phase of austenite. After cooling to 308 K, the martensitic transformation starts and the magnetization process changes, the typical step increase, which indicates the occurrence of MIR as mentioned above, is observed in the $M(H)$ loop, giving rise to a two-hysteresis loop. When temperature decreases to 300 K, the coercive force increases by a factor of 3 compared with the austenite at 315 K and further increases with decreasing temperature. This abrupt increase of coercivity is due to the higher magnetocrystalline anisotropy of martensite and the martensitic microstructure which is responsible for stronger pinning of domain walls. The MIR effect is first observed at the martensitic transformation starting temperature (Fig. 6(a)), 308 K. The switch field, H_s, increases remarkably in the temperature range of 308 K–300 K (Fig. 6(b)), resulting from the increasing volume of the martensitic phase with the progress of the martensitic transformation. With a further decrease of temperature, the hysteresis of the loop increases and the switching field is steadily shifted to higher values, a response that is also observed in the single crystal counterpart, consistent with an increase of the twinning stress due to damped thermal activation. This MIR effect persists down to 200 K.

To avoid the influence of thermal disturbance, magnetization curves of the film deposited at 873 K in the martensitic and austenitic state were recorded at the same temperature, 311 K, during heating and cooling (see in Fig. 3), respectively. Before measurements, the film was cooled and heated to 280 K and 350 K to obtain the fully martensitic and austenitic structure, respectively. Adopting the density of Ni–Mn–Ga bulk,[46] 8.04 g/cc, as that of Ni–Mn–Ga film deposited at 873 K, the magnetization is extracted with the unit of emu/g (Fig. 7(a)). The saturation magnetization of martensite under external field of 1.4 T is about 12% higher than that of austenite and it reaches 40.42 emu/g. Thus, the martensitic phase has a higher Zeeman energy than the austenitic phase at the same temperature if the film is magnetically saturated, resulting in a shift of martensitic transformation toward the high temperature phase, austenite, under a large magnetic field.

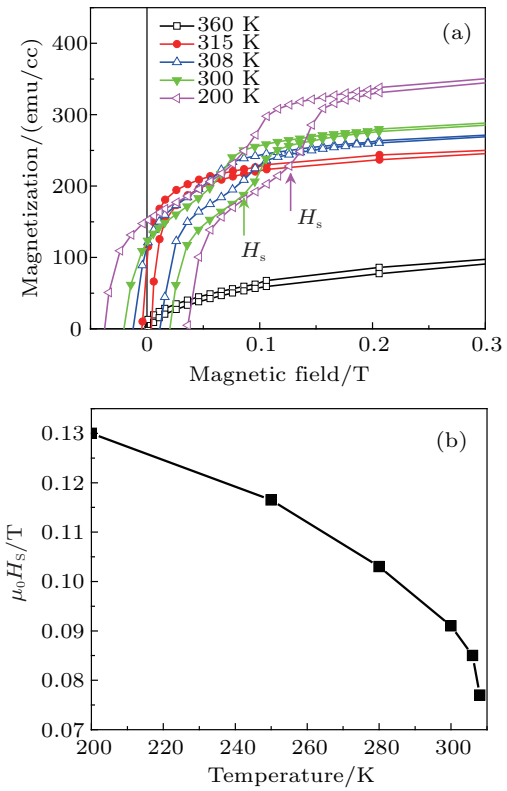


Fig. 6. (color online) (a) $M(H)$ loops recorded at 360, 315, 308, 300, and 200 K and (b) switching field, H_s, as a function of temperature for the Ni–Mn–Ga film deposited at 873 K.

Figure 7(b) exhibits the relation of the moment and the temperature for the Ni–Mn–Ga film deposited at 873 K under 0.01, 3, and 6 T during cooling. The martensitic transformation temperatures under magnetic fields of 0.01, 3, and 6 T are derived from thermomagnetization curves, as sketched in Fig. 7(b). When applying larger external magnetic fields, the martensitic transformation temperatures shift to higher values. A magnetic field stabilizes the martensite phase having a higher saturation magnetization M_M compared to austenite

M_A. This shift of transformation temperature ΔT can be calculated employing a generalized Clausius–Clapeyron equation,

$$dT/dH = \mu_0(M_M - M_A)T_M/Q,$$

where Q is the latent heat of the transformation and $T_M = (M_s + M_f)/2$ is the average thermodynamic martensitic transformation temperature. Using $T_M = 308$ K and a latent heat $Q = 5.5$ J/g,[47] a temperature shift is calculated to be 0.41 K/T, which is consistent with the experimental results, 0.43 K/T.

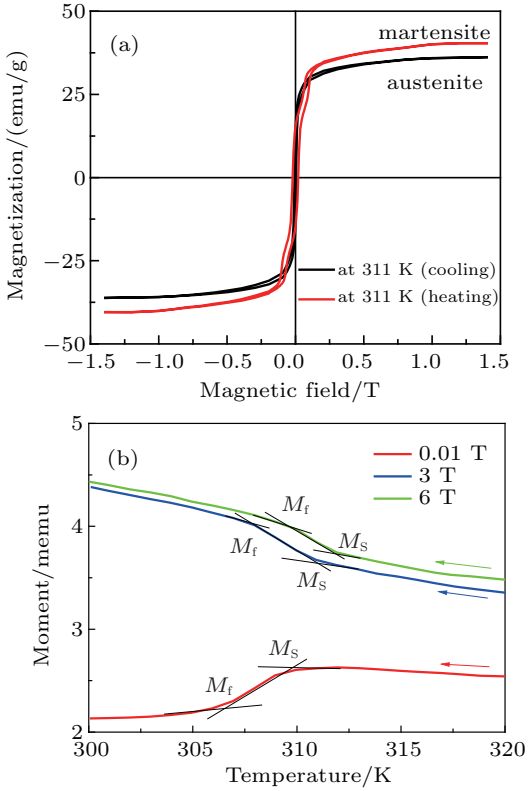


Fig. 7. (color online) (a) Magnetization curves recorded at 311 K during cooling and heating for the Ni–Mn–Ga film deposited at 873 K. (b) Relation of the moment and the temperature for the film deposited at 873 K cooling with magnetic fields of 0.01, 3, and 6 T.

4. Conclusion

In summary, ferromagnetic Ni–Mn–Ga films were prepared by deposition on MgO (001) from 673 K to 923 K. With deposition temperature increasing, the microstructure becomes denser and transforms from granular to integrated; a deposition temperature of 923 K results in coarse and coherent. The film deposited at 673 K is not fully crystallized; the films deposited at 773, 873, and 923 K have 5 M, 7M, and 2M martensitic structures, respectively. The film with 7M martensitic structure has the potential to realize MIR, which is reflected in the magnetization curve by a typical step-like increase. Deposition temperature has an only minor influence on transformation temperature; however, it produces distinct effects on transformation behavior as well as the crystal structure, which is attributed to the effect of the atomic order. An inter-martensitic transformation is observed in the Ni–Mn–Ga film deposited at 773 K. Transformation process could be divided into two periods: nucleation and growth. Two actuation modes, MIR and MIM, coexist in one film. The MIR occurs even when martensitic transformation starts, and the switch field increases with the decrease of temperature. The MIM originates from the difference in saturation magnetization between martensite and austenite. A shift of martensite temperature of dT/dH = 0.43 K/T is observed, consistent with the value 0.41 K/T calculated from a Clausius–Claperyon equation.

MIR is based on a coupling between microstructure and preferred magnetization direction. This coupling requires both intrinsic properties: high magnetocrystalline anisotropy and magnetization, and extrinsic properties, in particular a microstructure for the easy motion of twin boundaries. While MIM arises on account of the coupling of spontaneous magnetization of the phases, the effect is of significant magnitude only when the difference of the phases is large. No particular microstructure is required. The present film, deposited at 873 K, with continuous and smooth microstructure exhibits low mechanical friction for the motion of twin boundaries. It also displays high magnetization and noticeable difference of saturation magnetizations between austenite and martensite, allowing the coexistence of MIR and MIM.

References

[1] Liu Z H and Ma X Q 2012 *Acta Phys. Sin.* **61** 028103 (in Chinese)
[2] Banik S, Rawat R, Mukhopadhyay P K, Ahuja B L, Chakrabarti A, Paulose P L, Singh S, Singh A K, Pandey D and Barman S R 2008 *Phys. Rev. B* **77** 224417
[3] Opeil C P, Mihaila B, Schulze R K, Manosa L, Planes A, Hults W L, Fisher R A, Riseborough P S, Littlewood P B, Smith J L and Lashley J C 2008 *Phys. Rev. Lett.* **100** 165703
[4] Mandal K, Pal D, Scheerbaum N, Lyubina J and Gutfleisch O 2008 *IEEE Trans. Magn.* **44** 2993
[5] Cai P Y, Feng S S, Chen W P, Xue S X, Li Z G, Zhou Y, Wang H B and Wang G P 2011 *Acta Phys. Sin.* **60** 107501 (in Chinese)
[6] Ullakko K, Huang J K, Kantner C, O'Handley R C and Kokorin V V 1996 *Appl. Phys. Lett.* **69** 1966
[7] Wu G H, Yu C H, Meng L Q, Chen J L, Yang F M, Qi S R, Zhan W S, Wang Z, Zheng Y F and Zhao L C 1999 *Appl. Phys. Lett.* **75** 2990
[8] Sozinov A, Likhachev A A, Lanska N and Ullakko K 2002 *Appl. Phys. Lett.* **80** 1746
[9] Banik S, Ranjan R, Chakrabarti A, Bhardwaj S, Lalla N P, Awasthi A M, Sathe V, Phase D M, Mukhopadhyay P K, Pandey D and Barman S R 2007 *Phys. Rev. B* **75** 104107
[10] Karaca H E, Karaman I, Basaran B, Chumlyakov Y I and Maier H J 2006 *Acta Mater.* **54** 233
[11] Vasil'ev A N, Buchel'nikov V D, Takagi T, Khovailo V V and Estrin E I 2003 *Phys. Usp.* **46** 559
[12] Cai W, Liu C, Wang H B and Gao Z Y 2009 *J. Alloys Compd.* **468** 200
[13] Mahnke G J, Scibt M and Mayr S G 2008 *Phys. Rev. B* **78** 012101
[14] Wang H B, Liu C, Lei Y C and Cai W 2008 *J. Alloys Compd.* **465** 458
[15] Gao L, Sui J H and Cai W 2008 *J. Magn. Magn. Mater.* **320** 63
[16] Barandiaran J M, Gutierrez J, Lazpita P, Chernenko V A, Segui C, Pons J, Cesari E, Oikawa K and Kanomata T 2008 *Mater. Sci. Eng. A* **478** 125
[17] Sanchez-Alarcos V, Perez-Landazabal J I and Recarte V 2008 *Mater. Sci. Eng. A* **481** 293
[18] Ohtsuka M, Matsumoto M and Itagaki K 2006 *Mater. Sci. Eng. A* **438** 935

[19] Khol M, Brugger D, Ohtsuka M and Takagi T 2004 *Sens. Act. A* **114** 445

[20] Tello P G, Castano F J, O'Handley R C, Allen S M, Esteve M, Castano F, Labarta A and Batlle X 2002 *J. Appl. Phys.* **91** 8234

[21] Dong J W, Chen L C, Palmstrom C J, James R D and McKernan S 1999 *Appl. Phys. Lett.* **75** 1443

[22] Dong J W, Xie J Q, Lu J, Adelmann C, Palmstrom C J, Cui J, Pan Q, Shield T W, James R D and McKerman S 2004 *J. Appl. Phys.* **95** 2593

[23] Chernenko V A, Khol M, Doyle S, Müllne P and Ohtsuka M 2006 *Scr. Mater.* **54** 1287

[24] Khol M, Agarwal A, Chernenko V A, Ohtsuka M and Seemann K 2006 *Mater. Sci. Eng. A* **438** 940

[25] Sozinov A, Likhachev A A and Ullakko K 2002 *IEEE Trans. Magn.* **38** 2814

[26] Besseghini S, Gambardella A, Chernenko V A, Hagler M, Pohl C, Müllner P, Ohtsuka M and Doyle S 2008 *Eur. Phys. J.* **158** 179

[27] Chernenko V A, Ohtsuka M, Kohl M, Khovailo V V and Takagi T 2005 *Smart Mater. Struct.* **14** S245

[28] Doyle S, Chernenko V A, Besseghini S, Gambardella A, Kohl M, Müllner P and Ohtsuka M 2008 *Eur. Phys. J.* **158** 99

[29] Heczko O, Thomas M, Niemann R, Schultz L and Fähler S 2009 *Appl. Phys. Lett.* **94** 152513

[30] Thomas M, Heczko O, Buschbeck J, Schultz L and Fähler S 2008 *Appl. Phys. Lett.* **92** 192515

[31] Song R N, Zhu W, Liu E K, Li G J, Chen J L, Wang W H, Li X and Wu G H 2012 *Acta Phys. Sin.* **61** 027501 (in Chinese)

[32] Annadurai A, Nandakumar A K, Jayakumar S, Kannana M D, Raja M M, Bysak S, Gopalan S and Chandrasekaran V 2009 *J. Magn. Magn. Mater.* **321** 630

[33] Annadurai A, Raja M M, Prabahar K, Kumar A, Kannan M D and Jayakumar S 2011 *J. Magn. Magn. Mater.* **323** 2797

[34] Chmielus M, Zhang X X, Witherspoon C, Dunand D C and Müllner P 2009 *Nat. Mater.* **8** 863

[35] Chmielus M, Rolfs K, Wimpory R, Reimers W, Müllner P and Schneider R 2010 *Acta Mater.* **58** 3952

[36] Zhang Y P, Hughes R A, Britten J F, Gong W H, Preston J S, Botton G A and Niewczas M 2009 *Smart Mater. Struct.* **18** 025019

[37] Pons J, Chernenko V A, Santamarta R and Cesari E 2000 *Acta Mater.* **48** 3027

[38] Segu C, Pons J and Cesari E 2007 *Acta Mater.* **55** 1649

[39] Ishikawa H, Umetsu R Y, Kobayashi K, Fujita A, Kainuma R and Ishida K 2008 *Acta Mater.* **56** 4789

[40] Thomas M, Heczko O, Buschbeck J, Rößler U K, McCord J, Scheerbaum N, Schultz L and Fähler F 2008 *New J. Phys.* **10** 023040

[41] Heczko O, Thomas M, Buschbeck J, Schultz L and Fähler S 2008 *Appl. Phys. Lett.* **92** 072502

[42] Zhang Y P, Hughes R A, Britten J F, Preston J S, Botton G A and Niewczas M 2010 *Phys. Rev. B* **81** 054406

[43] Buschbeck J, Niemann R, Heczko O, Thomas M, Schultz L and Fähler S 2009 *Acta Mater.* **57** 2516

[44] Neudert A, Lai Y W, Schäfer R, Kustov M, Schultz L and McCord J 2012 *Adv. Eng. Mater.* **14** 601

[45] Lai Y W, Schäfer R, Schultz L and McCord J 2010 *Appl. Phys. Lett.* **96** 022507

[46] Righi L, Albertini F, Pareti L, Paoluzi A and Calestani G 2007 *Acta Mater.* **55** 5237

[47] Scheerbaum N, Heczko O, Liu J, Hinz D, Schultz L and Gutfleisch O 2008 *New J. Phys.* **10** 073002